Assessment of Ionospheric Correction Behavior for Use with Precise Point Positioning (PPP)

Todd Walter, *Stanford University*
Juan Blanch, *Stanford University*
Lance de Groot, *Hexagon Autonomy and Positioning*
Laura Norman, *Hexagon Autonomy and Positioning*

ABSTRACT

Stanford and Hexagon performed this analysis to assess the accuracy and behavior of ionospheric corrections provided for use with Precise Point Positioning (PPP). In particular we are interested in the achieved level of precision as a function of ionospheric state, reference correction message latency, and network location and coverage. In this study we analyze 28 days' worth of data from three different locations within North America. The data is from April 2020 and the locations include Priddis in Alberta, and Stanford and Vandenburg in California. Correction data is applied to IGS reference station data from these three locations.

Double difference evaluations were formed by comparing the measurements minus the estimated ionosphere for one satellite against the measurements minus the estimated ionosphere for another. These double differences demonstrated precision to the level of 2 cm 95% across the entire period with little day to day variation. The accuracy degraded very slowly with latency and did not exhibit noticeable increase in the error until 120 seconds of latency was applied. By 240 seconds the 95% containment had increased to 3 cm. This weak dependency on latency is most likely due to the fact that 2020 is near the very lowest point of solar minimum conditions and the ionospheric variability is also minimized.

We are also very interested in bounding these ionospheric errors. A confidence sigma was provided along with the outliers of the corrections and we evaluate the normalized distribution as well. We examined the full distribution of both the corrections errors and normalized correction errors in order to assess the trustworthiness of the corrections and to determine the probability that the provided sigma value will not sufficiently describe the expected error distribution.

INTRODUCTION

Hexagon is investigating the utility of applying ionospheric corrections in order to decrease the overall convergence time of the PPP filter [1]. Stanford University has conducted several analyses on the accuracy of these ionospheric corrections over the course of the past two years. Stanford has created MATLAB tools to process data from multiple days and locations as well as to investigate intervals with larger disagreements between the raw ionospheric measurements and the provided corrections. In addition, the tool can apply varying magnitudes of latency in order to examine its effect on correction accuracy and error bounding.

The current study was performed using data from April 12 – May 9, 2020. These days exhibit typical ionospheric behavior for a solar minimum period. Hexagon provided 1 Hz correction data for three International GNSS Service (IGS) sites in order to evaluate their accuracy. These sites are Stanford University (IGS 4-letter identifier: STFU), Vandenberg Air Force Base (VNDP) in southern California, and Priddis, Alberta (PRDS). These sites were chosen because they tend to have high volumes of good quality data and are covered by the ionospheric correction service.

The provided corrections were specifically calculated for the three reference sites listed above. They include corrections for GPS and GLONASS satellites. We downloaded RINEX data for the three sites for all 28 days from IGS. All three sites contain raw GPS and GLONASS data. The Stanford site provides 1 Hz data, VNDP has measurements at every 15 seconds, and PRDS has measurements every 30 seconds. Figure 1 shows the locations of the three sites.

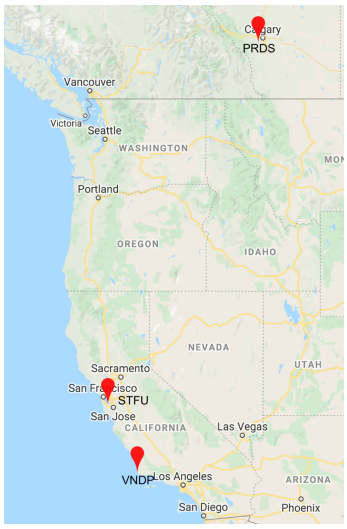

Figure 1. The 3 station locations

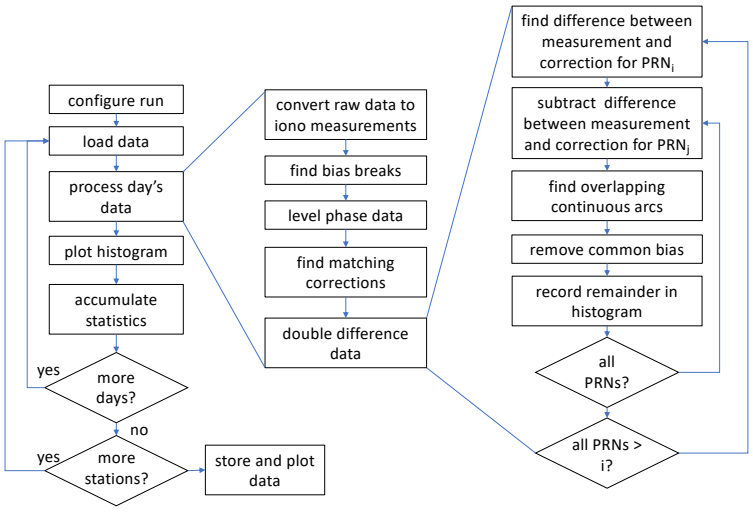

Figure 2. The processing flowchart

PROCESSING METHODOLOGY

The residual errors were determined by comparing the measured ionosphere to the corrections for all satellites. These differences contain a common mode effect due to the changing inter-frequency biases that are part of the corrections. We formed double differences for all satellite pairs (within each constellation) that have measurements and corrections present at the same time. For each such pair, the continuous tracks are determined and a constant offset for each continuous track is subtracted to obtain the final residual error. This process is illustrated in the flowchart shown in Figure 2 as well as in the following example. Figure 3 shows the raw ionospheric measurements for PRNs 03and 31. The blue +'s use the L2 minus L1 code measurement difference divided by $(\gamma - 1)$ where γ is the square of the ratio of the carrier frequencies ($f_1^2/f_2^2 \cong 1.65$). The green circles are the L1 code minus the L1 carrier divided by two and the red dots are the L1 minus L2 carrier measurement difference divided by $(\gamma - 1)$. The different measurements are formed to help identify erroneous measurements that might corrupt the evaluation. Fortunately, the vast majority of the measurement data is well behaved. The traces shown in Figure 3 are all self-consistent and indicative of valid measurement data. The carrier phase difference measurements are then used in the remainder of the processing as these have the least amount of measurement noise.

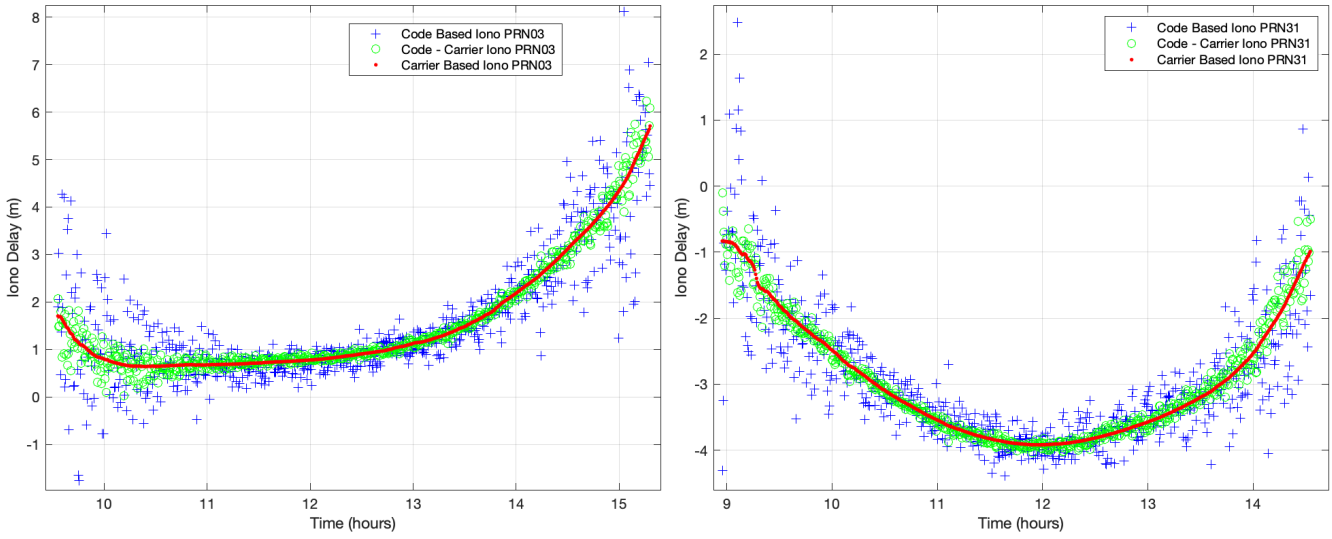

Figure 3. Raw Ionospheric measurements for GPS PRNs 03 (left) and 31(right)

In the left side of Figure 4 we present the carrier phase ionospheric delay measurements of PRNs 03 and 31 alongside their corresponding corrections. The middle section of the figure shows the differences between measured and estimated correction values for each satellite. Notice that there are common mode drifts that span ~50 cm for this particular example. Finally, the right side of Figure 4 shows the difference between the two curves in the middle portion. This double difference is the difference between these two corrected satellites for the periods of time that they are simultaneously observed by each reference station. For each continuous double difference track (i.e., that has no detected bias break), we subtract out the mean value (provided that the track spans at least four minutes). We examine this residual error in meters and the normalized residual error where we divide by the RSS of the provided correction one-sigma values. The process begins by comparing PRNs 1 & 2, then comparing PRNs 1 & 3 and so on until PRN 31 has been compared to PRN 32. We then repeat the same process for the GLONASS PRNs.

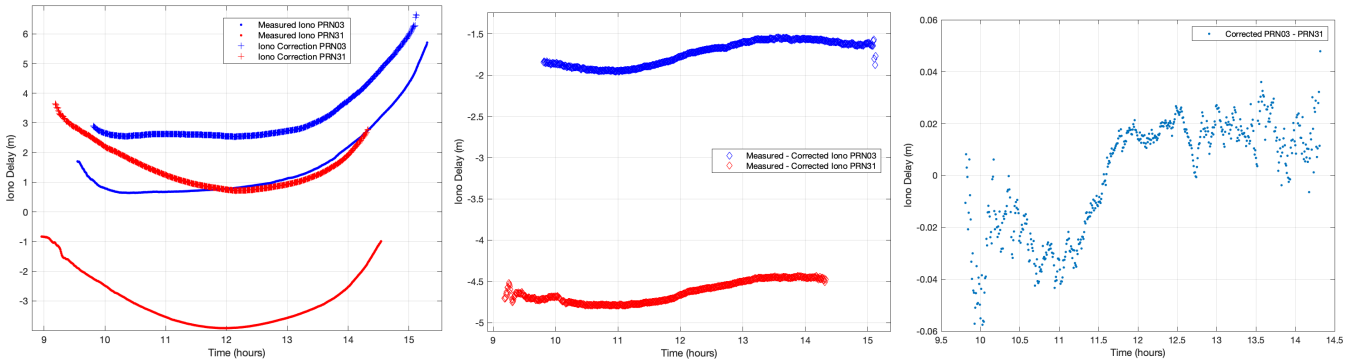

Figure 4. Ionospheric measurements and corrections for GPS PRNs 03 and 31(left), differences between the measurements and corrections (middle) and double differences between the satellite pair (right)

These values are put into histograms and the 95%, 99.9% and 99.999% quantiles are determined for each metric. These are calculated on a daily basis across all satellite pairs as well as aggregated over multiple days and stations. By comparing different quantile behaviors, we can see whether the full distributions are close to Gaussian (well behaved) or if they have outliers which create large tail values (poorly behaved). Figure 5 shows the histograms of data for the Stanford University station for the first day analyzed.

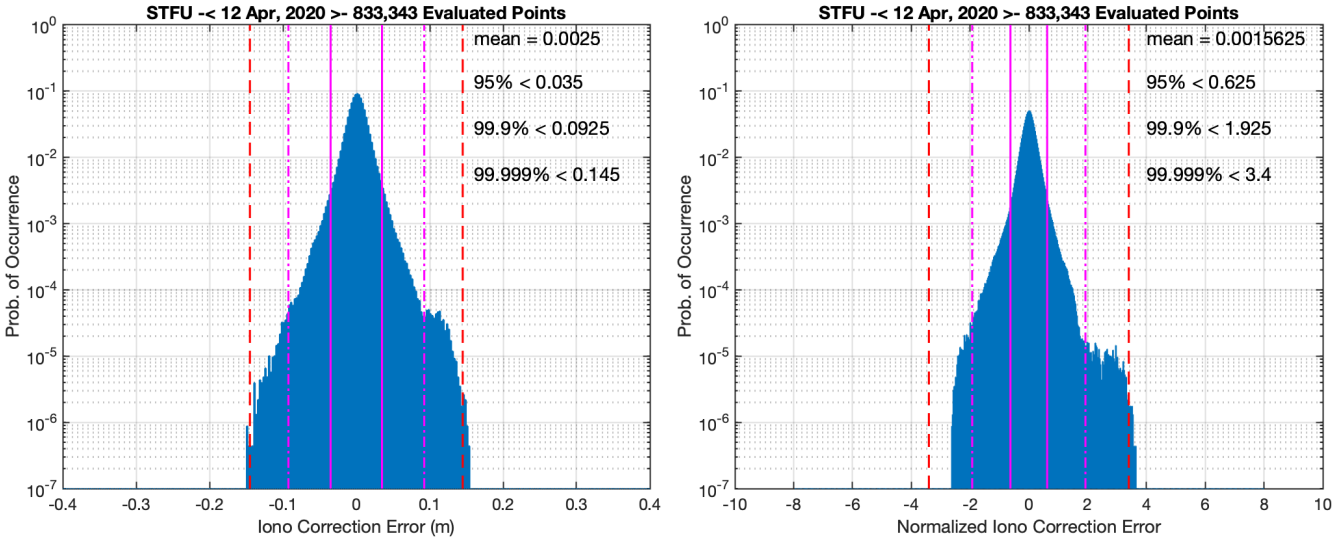

Figure 5. Histogram of double differenced residual error at Stanford (left) and normalized error (right)

As can be seen, the data is very well behaved (the histograms are plotted on a semi log scale to emphasize the performance of the tails. If the data strictly followed a Gaussian distribution, we would expect that 95% would fall within 2 σ, 99.9% within

3.29 σ, and 99.999% within 4.42 σ. Very often similar data would have much wider tails and include many outliers, however this data has only slightly wider tails than would be expected for a Gaussian distribution. The double difference includes the noise from two sets of measurements and two different corrections. The values in the right side of Figure 5 should be divided by the square root of 2 in order to assess the magnitude of error affecting just one satellite. The values on the left histogram use the square root of the sum of the variances associated with the corrections, so no similar adjustment is required there.

Figure 6 shows the results of evaluating the Stanford station over all 28 days. Here the 95%, 99.9%, 99.999% and maximum values are shown for each individual day. The 95% values are fairly consistent over the 28-day period, but there is more variability in the tails of these distributions. Figure 7 shows the same data for Vandenburg and Figure 8 has the data for Priddis. Note that the errors are largest for Vandenburg with is situated near the edge of coverage for the corrections. Priddis has the smallest errors which is likely due to good network coverage and smaller ionospheric delays nearer to the Earth's polar regions.

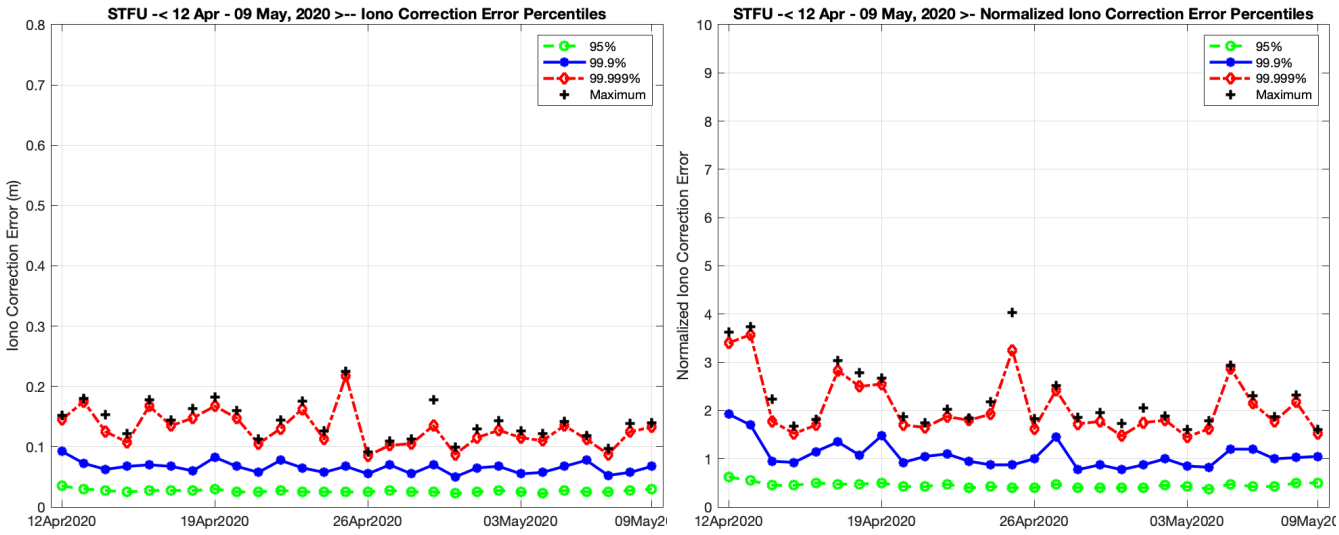

Figure 6. Ionospheric corrections accuracy quantiles for GPS and GLONASS at Stanford from April 12 – May 9, 2020. *Ionospheric delay double differenced residuals (left) and normalized values (right).*

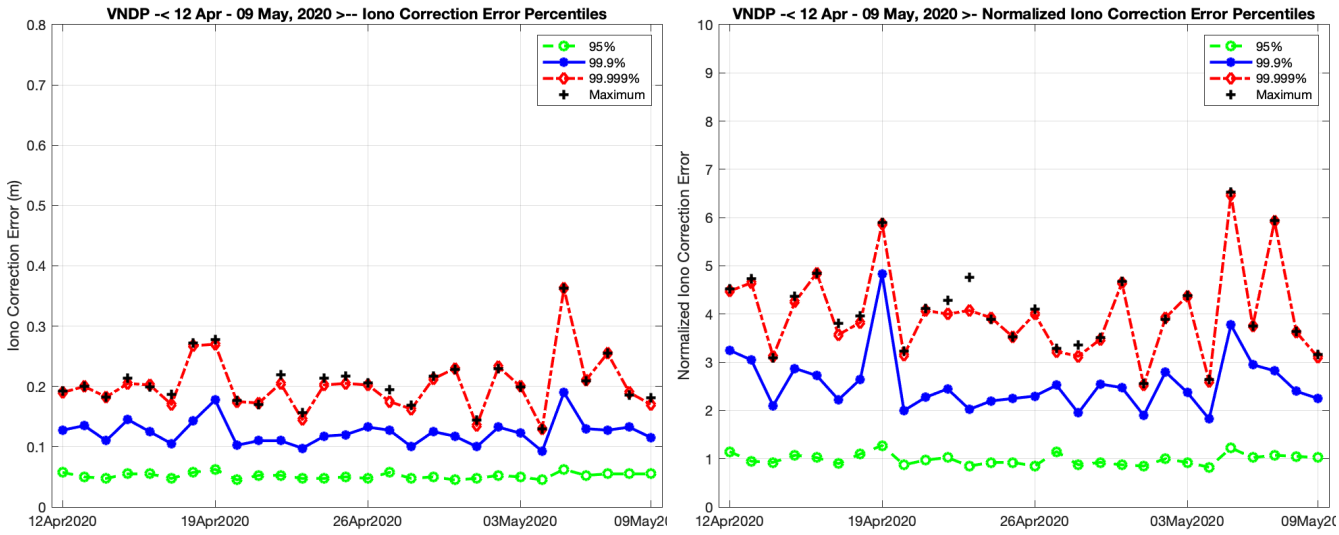

Figure 7. Ionospheric corrections accuracy quantiles for GPS and GLONASS at Vandenburg from April 12 – May 9, 2020. *Ionospheric delay double differenced residuals (left) and normalized values (right).*

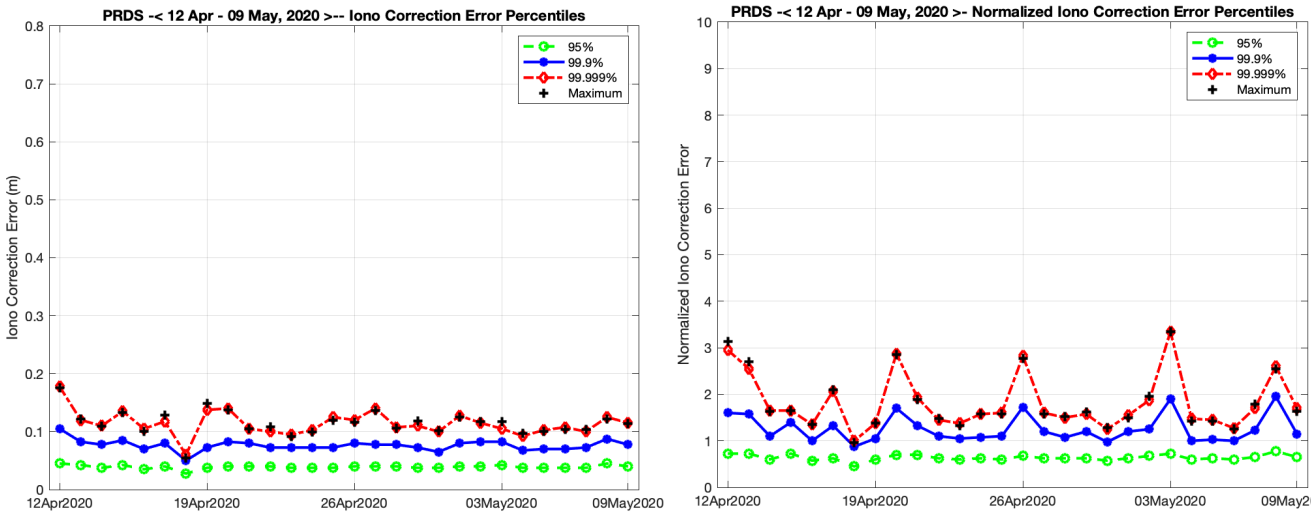

Figure 8. Ionospheric corrections accuracy quantiles for GPS and GLONASS at Priddis from April 12 – May 9, 2020. *Ionospheric delay double differenced residuals (left) and normalized values (right).*

Figure 9 shows the aggregate histograms for all of the data across the three stations for the full 28 days. The accuracy of these corrections for the vast majority of the data remains quite impressive, the 95% value indicates a 1-σ accuracy of ~1 cm $\left(3\ cm/2\sqrt{2}\right)$. The higher quantiles indicate slightly larger values due to the wider tails of the distribution with the 99.9% indicating a 1-σ of ~1.7 cm $\left(8\ cm/3.29\sqrt{2}\right)$ and the 99.999% indicating a 1-σ of ~2.9 cm $\left(18\ cm/4.42\sqrt{2}\right)$. The provided error bounds are conservative for most of the data. For 95% they are four times larger than necessary and for 99.9% two times larger. However, by 99.999%, they are only 10% larger than strictly necessary and are insufficient for even smaller probabilities. This highlights the larger tail behavior and that the error bounds which are currently only a function of elevation angle, should be updated to reflect more information about the transformation of the reference measurements into the estimate of ionospheric delay. Corrections near to the edge of coverage or that make use of fewer and/or less accurate measurements would be expected to have larger error bounds.

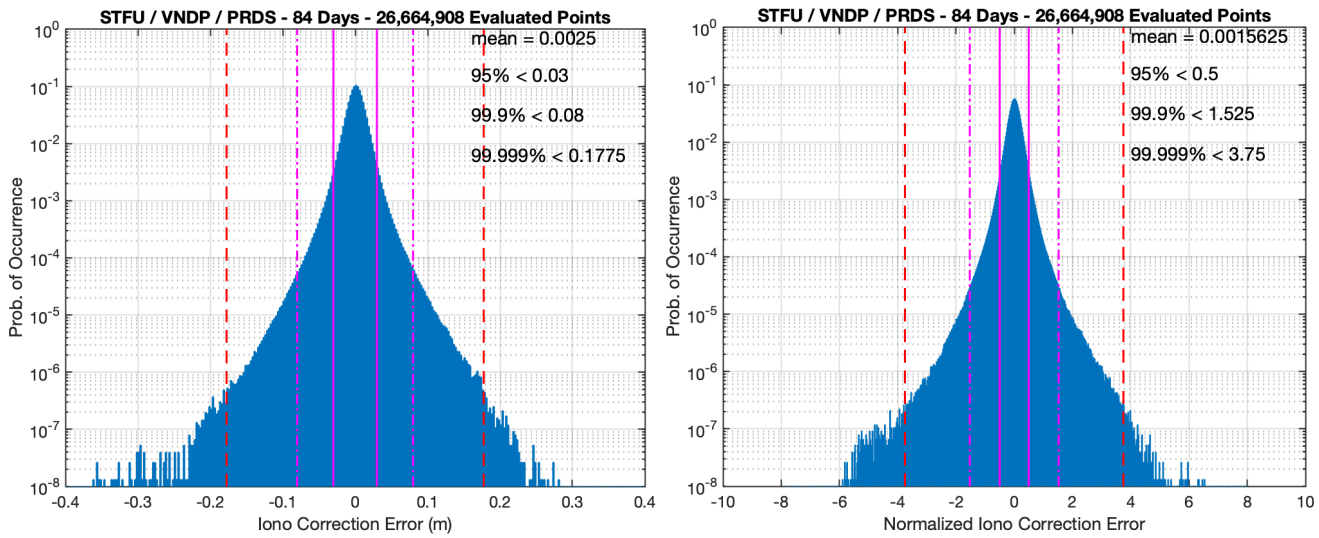

Figure 9. Ionospheric correction histograms for GPS and GLONASS at all three sites from April 12 – May 9, 2020. *Ionospheric delay double differenced residuals (left) and normalized values (right).*

COMPARISON TO KLOBUCHAR CORRECTIONS

We are currently at a solar minimum period and the ionospheric delays are both smaller and smoother than are typically experienced during other phases of the ionospheric solar cycle. To demonstrate that the corrections are accurately following the ionospheric behavior and that the demonstrated accuracy is not merely a reflection of extremely smooth ionosphere, we repeated the same process using the single frequency global ionospheric model broadcast by the GPS satellites [2]. This model is commonly referred to as the Klobuchar model. Figure 10 uses the same measurement data as Figure 9, but now the corrections are replaced with the Klobuchar model from each day and the error bound is set to a constant 1 m 1-σ value. As can be seen the error magnitude is significantly increased to values of 50 - 60 cm 1-σ. Thus, the provided corrections are very accurately following the ionospheric behavior to within a few cm and the actual variations in the ionosphere are more than an order of magnitude larger.

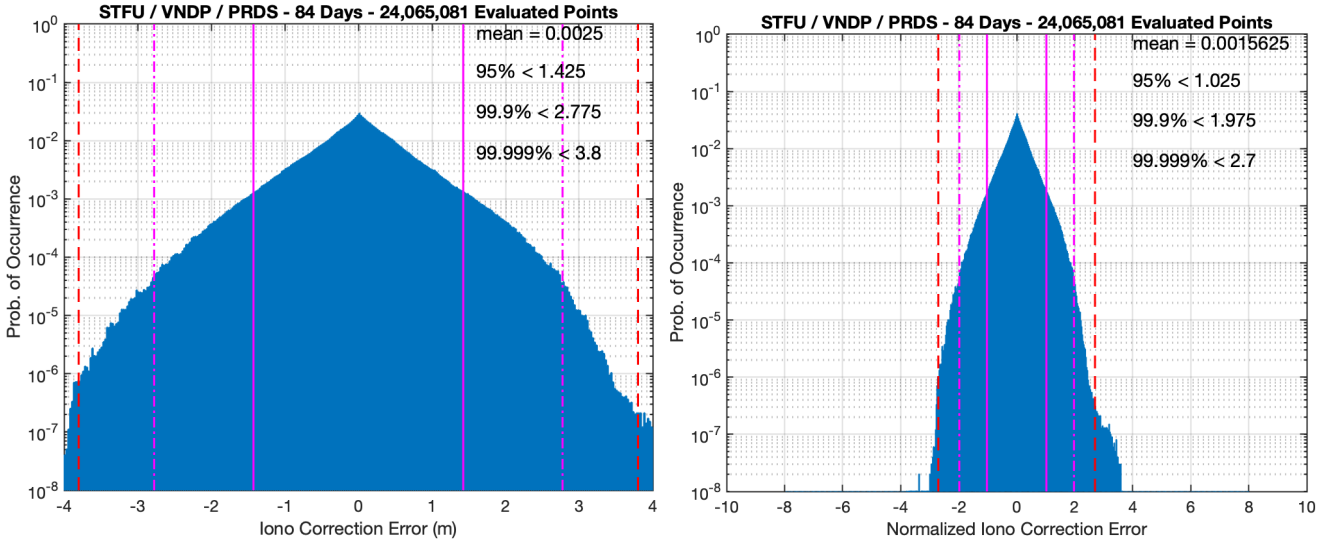

Figure 10. Klobuchar correction histograms for GPS and GLONASS at all three sites from April 12 – May 9, 2020. *Ionospheric delay double differenced residuals (left) and normalized values (right).*

In order to examine the changes in ionospheric variability over the solar cycle, we examined four Eastern stations during a significant ionospheric disturbance on October 29, 2003. These stations are in Bermuda, Greenbelt Maryland, Santiago de Cuba, Cuba, and Washington DC. They experienced some very large ionospheric gradients during that event [3]. Figure 11 shows similar data for the four stations from that day. Note that the x-axis for each graph had to be expanded to include all of the errors. Here the errors are between 2.8 and 7.4 m 1-σ.

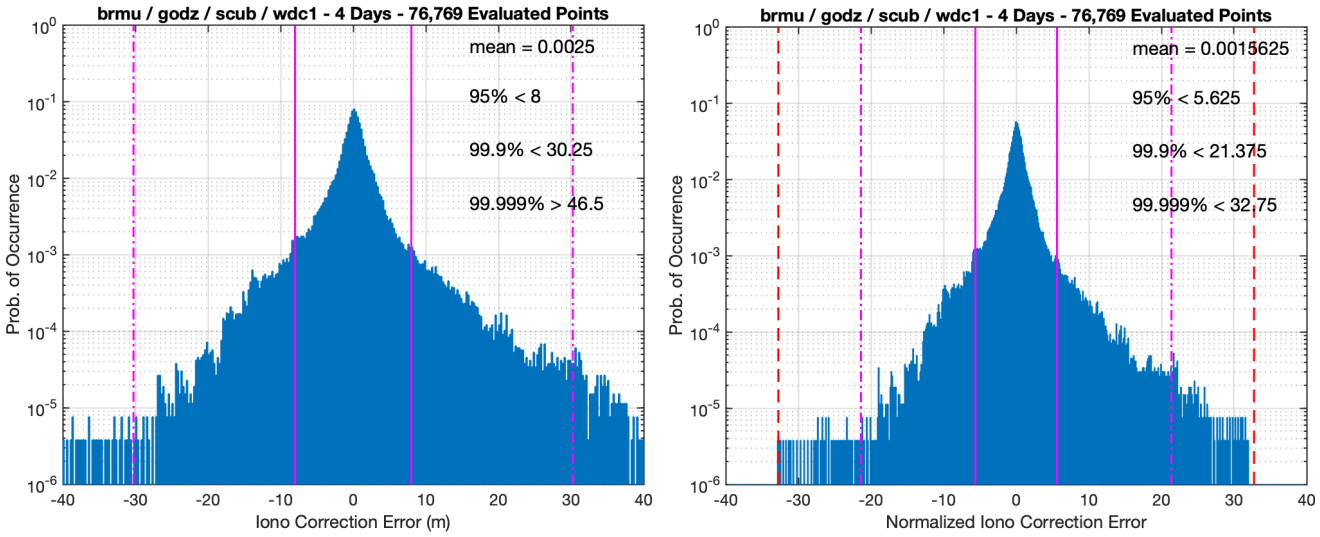

Figure 10. Klobuchar correction histograms for GPS and GLONASS at all three sites from April 12 – May 9, 2020. *Ionospheric delay double differenced residuals (left) and normalized values (right).*

EVALUATION OF THE EFFECTS OF LATENCY

We are able to configure the tool to implement different levels of latency for the corrections. This is configured as a minimum age for the corrections before they can be applied to the measurements. In all cases, the maximum age of the data beyond the initial latency value was set to 30 seconds. For example, when set to 60 seconds of latency, corrections had to be at least 60 seconds old in order to apply to the current epoch. If no correction existed that was between 60 and 90 seconds old, then the measurement would not be corrected.

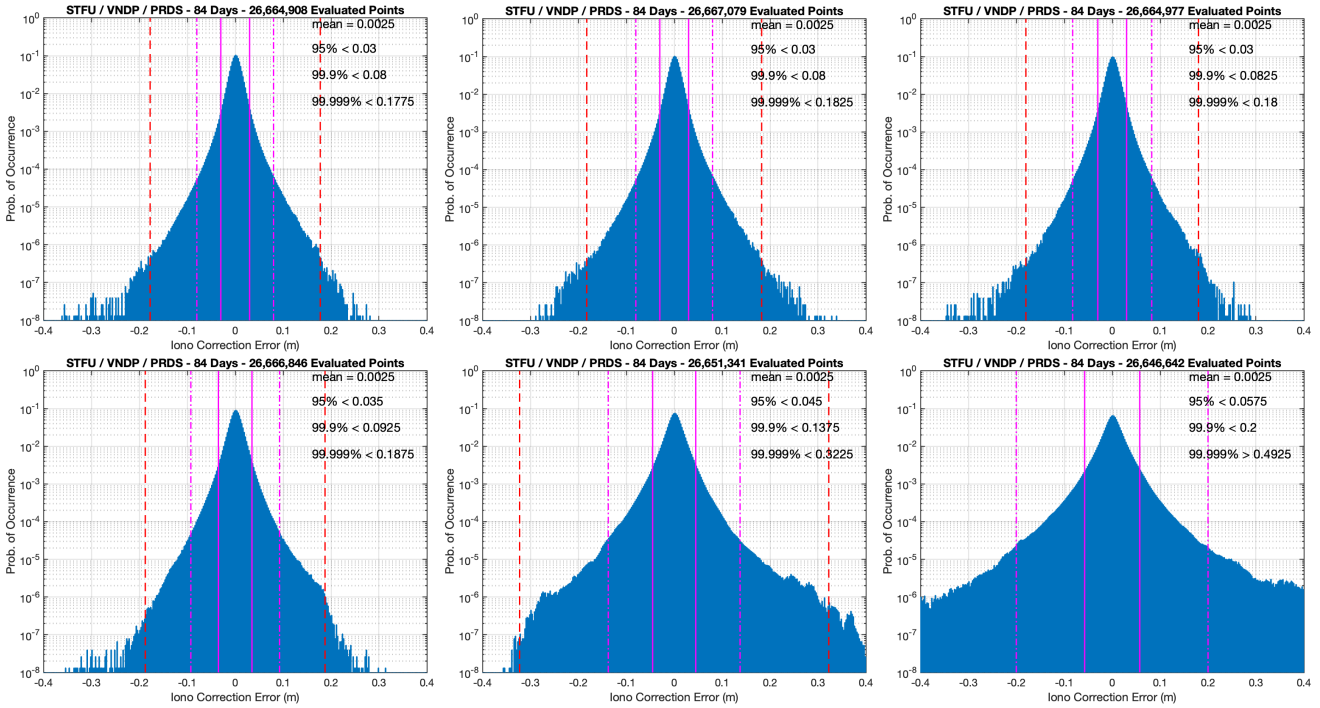

Figure 11. Histograms showing the double difference residual accuracy for differing amounts of latency From left to right:
Top Row: 0 sec, 30 sec, and 60 sec
Bottom Row: 120 sec, 240 sec, and 360 sec

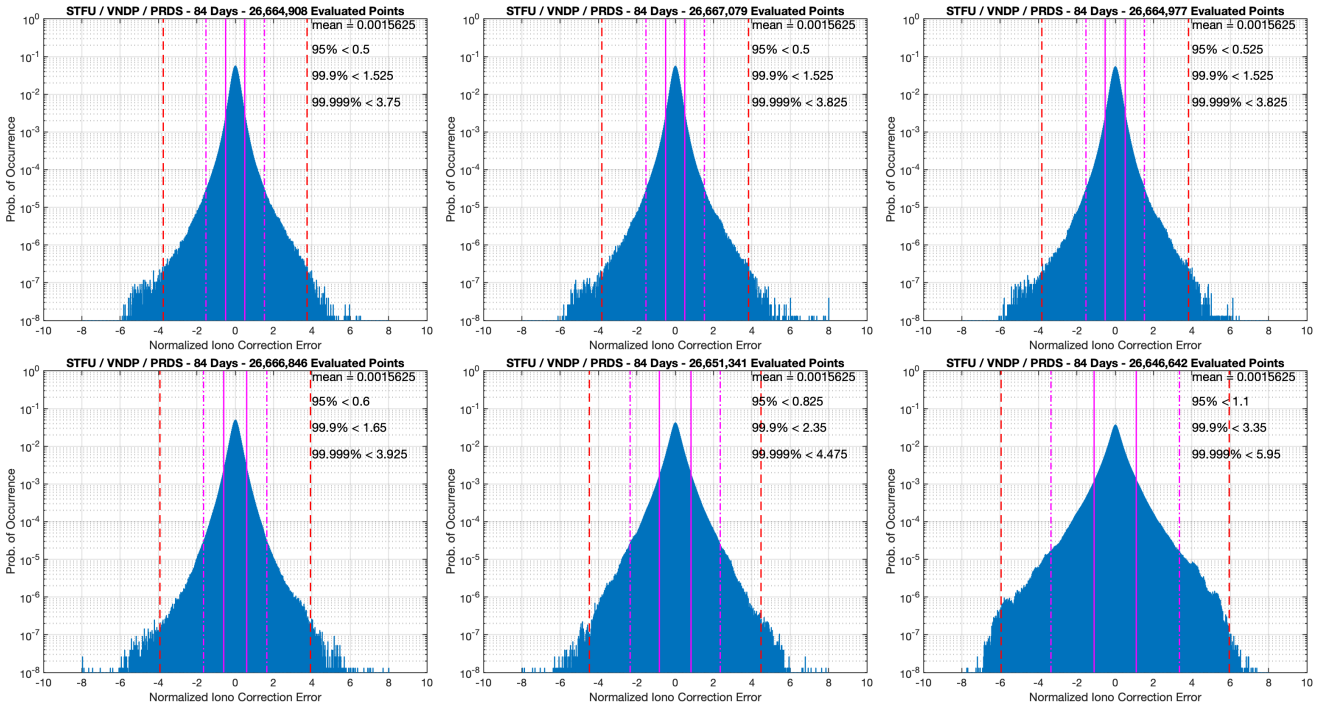

Figure 12. Histograms showing the normalized double difference residual for differing amounts of latency
From left to right: Top Row: 0 sec, 30 sec, and 60 sec
Bottom Row: 120 sec, 240 sec, and 360 sec

Figures 11 and 12 show results for this latency study. The top row of each corresponds to 0, 30, and 60 seconds from left to right. There was surprisingly little effect for this range of latencies, most likely due to the very benign ionosphere during the current Solar Minimum period. The accuracy quantiles only increased by less than half of a centimeter over this period. The normalized errors saw somewhat larger growth, but the sigma values are still appropriately bounding the errors. The bottom rows correspond to 120, 240, and 360 seconds of latency, from left to right. Here we begin to see more effect from latency, the residual error is doubled by 360 seconds. Between, 240 and 360 seconds, the 99.999% normalized residual error exceeds 4.42 which corresponds to the expected Gaussian value. We can also see more outliers beyond six-sigma.

We fit the quantiles vs. the latency times and found a strong quadratic dependence. Table 1 shows the resulting growth rates for the overall error and the 1-σ values for each quantile. For the observed level of ionospheric activity, we recommend adding an increase to the one-sigma confidence value as a function of the age of the correction. We recommend an added value of 4.5×10^{-5} cm/sec^2, thus after 200 seconds the one-sigma value should be increased by 1.8 cm. However, for solar maximum periods and during significant ionospheric disturbances [4] we feel that this error bound will need to be increased, perhaps significantly. This error bound term should be linked to the state of the ionosphere.

Table 1. Ionospheric Correction Error Growth Rates

Quantile	Error Growth	One Sigma Value
95%	10^{-5} cm/sec^2	5×10^{-6} cm/sec^2
99.9%	6×10^{-5} cm/sec^2	1.9×10^{-5} cm/sec^2
99.999%	2×10^{-4} cm/sec^2	4.5×10^{-5} cm/sec^2

CONCLUSIONS

The correction accuracy is generally quite good, with 95% daily values almost always below 4 cm and below 6.25 cm overall. There are, however, outliers that affect the daily 99.9% and 99.999% percentiles particularly at Vandenburg which is towards the edge of the correction coverage region. The provided error bounds are mostly very conservative, but there were

still some occasional outliers. These error bounds should be more than simply functions of elevation angles. They should include real-time updates on the state of the ionosphere and quality of the correction based on the input measurements.

We evaluated the effects of latency and found that during this solar minimum period fairly long latency times (up to 120 seconds) showed very little impact to performance and it was not until more than 240 seconds that the sigma values stopped adequately bounding the tails and the overall accuracy degraded appreciably. We advocate including a quadratic term to the error bound to account for the age of the correction. During solar minimum time we observed that this term can be quite small (4.5×10^{-5} cm/s^2), but anticipate it needing to be significantly larger during times of ionospheric disturbance.

REFERENCES

[1] https://hexagonpositioning.com/autonomous-x/automotive-positioning/serial-production/correction-services

[2] Klobuchar, J., 1987. "Ionospheric Time-Delay Algorithms for Single-Frequency GPS Users." IEEE Transactions on Aerospace and Electronic Systems (3), pp. 325-331.

[3] Walter, Todd, Blanch, Juan, DeGroot, Lance, Norman, Laura, Joerger, Mathieu, "Ionospheric Rates of Change," Proceedings of the 31st International Technical Meeting of the Satellite Division of The Institute of Navigation (ION GNSS+ 2018), Miami, Florida, September 2018, pp. 4158-4170.
https://doi.org/10.33012/2018.16112

[4] Sparks, Lawrence, Altshuler, Eric, "Ionospheric Storms of Solar Cycle 24 and their Impact on the WAAS Ionospheric Threat Model," Proceedings of the 29th International Technical Meeting of the Satellite Division of The Institute of Navigation (ION GNSS+ 2016), Portland, Oregon, September 2016, pp. 682-690.
https://doi.org/10.33012/2016.14850